Measuring Coexisting Densities from a Two-Phase Molecular Dynamics Simulation by Voronoi Tessellations

Jared T. Fern,[†] David J. Keffer,[*,†] and William V. Steele[†,‡]

Physical Properties Research Facility, Chemical Engineering Department, 327 Dougherty Engineering Building, University of Tennessee, 1512 Middle Drive, Knoxville, Tennessee 37996-2200, and Nuclear Science and Technology Division, Oak Ridge National Laboratory (ORNL), Oak Ridge, Tennessee 37831-6273

Received: November 10, 2006; In Final Form: January 12, 2007

A new algorithm is presented that allows for the determination of bulk liquid and vapor densities from a two-phase Molecular Dynamics (2ϕMD) simulation. This new method does not use any arbitrary cutoffs for phase definitions; rather it uses single-phase simulations as a self-consistency check. The method does not use any spatial bins for generating histograms of local properties, thereby avoiding the statistical issues associated with bins. Finally, it allows one to approach very close to the critical point. The new method utilizes Voronoi tessellations to determine the molecular volume of every point at every instance in a molecular dynamics simulation. Since the molecular volume is calculated throughout the simulation, statistical parameters such as the average molecular volume and average molecular variance are easy to obtain. To define the phases, the normalized variance of the molecular volume from 1ϕMD and 2ϕMD is used as a self-consistency check. The new method gives new insight into the nature of the near-subcritical fluid. The critical properties from this analysis are $T_c = 1.293$ and $\rho_c = 0.313$. Direct simulation of the two-phase system was performed up to a temperature of 1.292. The results show excellent agreement to experimental results and Gibbs Ensemble Monte Carlo for coexisting densities. We see that well below the critical temperature, some particles are neither liquid nor vapor. These interfacial particles are primarily, but not exclusively, concentrated at the bulk interface. However, as we approach the critical point, some particles are considered both liquid and vapor. These interfacial particles are distributed through the system.

Introduction

There are a variety of tools available for the study of Vapor−Liquid Equilibrium (VLE). Aside from experimental measurements, computational methods have been evolving since the mid 1970s.[1,2] Ladd and Woodcock and Chapela et al. studied VLE by simulating a slab of a liquid and a slab of a vapor to find the surface tension and the equilibrium densities by Molecular Dynamics (MD). The work of Ladd and Woodcock was then extended upon by Holcomb et al.[3,4]

Along with these examples for MD simulations, there are many additional ways to simulate VLE. One common method to study phase equilibrium is by Gibbs Ensemble Monte Carlo (GEMC).[5,6] GEMC simulates the bulk liquid and bulk vapor in separate boxes and the molecules are allowed to exchange between the boxes. The simulation strives to maintain a constant chemical potential, temperature, and pressure between the two boxes. One other method of direct simulation of vapor liquid equilibrium is the NPT + test particle method created by Lofti and co-workers.[7] The method is implemented by conducting a MD simulation in the isothermal−isobaric ensemble (NPT) coupled with the Widom particle insertion method[8] to obtain the chemical potential of the system. Simulations are performed for both the liquid and vapor phases independently and the results are then used to calculate the points on the two-phase envelope.

There are also indirect methods to obtain phase equilibrium. These indirect methods use an established state point and then use statistical methods to obtain the rest of the two-phase region close to the critical point. These methods include histogram reweighting techniques[6,9,10] and Gibbs−Duhem integration.[6]

The two primary methods available to directly simulate the phase diagram are two-phase Molecular Dynamics (2ϕMD) and GEMC. There are known deficiencies with the GEMC methods as mentioned by Gelb and Müller.[11] Equilibration is difficult to achieve when simulating dense phases because of the poor statistics associated with the insertion/deletion steps. The GEMC methods are difficult to apply to systems containing very complex molecules without substantial modifications, and are also difficult to implement on parallel computers. In addition to these deficiencies, GEMC simulations can have problems as the simulation approaches the critical temperature because the identity of the volumes can swap during the simulation.[6] When this occurs the results are then analyzed by the distribution of a given density in the simulation.

Simulating VLE with MD in the canonical (NVT) ensemble can potentially overcome all of the limitations of GEMC. In addition, complex fluids are routinely handled and MD codes are particularly amenable to parallelization. Perhaps more importantly, by simulating the interface, MD simulations allow for the investigation of interfacial properties such as molecule orientation, diffusion of molecules through the interface, and

* Author to whom corrrespondence should be addressed. E-mail: dkeffer@utk.edu. Phone: (865)-974-5322.
† University of Tennessee.
‡ Oak Ridge National Laboratory.

10.1021/jp0674470 CCC: $37.00 © xxxx American Chemical Society
Published on Web 03/09/2007 PAGE EST: 6.4

thickness of the interface. Furthermore, one can observe the dynamics of interface formation and destruction in MD simulations.

In the past few years, there have been two different ways developed to study VLE with MD. These two methods are Temperature Quench Molecular Dynamics (TQMD) and Volume Expansion Molecular Dynamics (VEMD). TQMD, as implemented by Gelb and Müller,[11] allowed for the simulation of the liquid and vapor phases in the same simulation cell. The system is equilibrated at a temperature above the critical temperature and density then suddenly cooled to a region of mechanical and thermodynamic instability. The system then separates into liquid and vapor phases separated by an interface. VEMD, used by Pamies et al.,[12] also allowed for the simulation of the vapor and liquid phases to be simulated in the same cell. This method is analogous to a piston experiment where a volume of liquid is suddenly expanded to give liquid and vapor phases. The VEMD model starts as an equilibrated liquid then the simulation cell is suddenly expanded to give a density in the unstable region along the line of rectilinear diameters. The system then separates into vapor and liquid phases separated by an interface.

The above methods are two different ways to obtain a two-phase system by molecular dynamics. The more difficult task associated with 2ϕMD (and absent in low-temperature GEMC) is extracting the values for the bulk liquid and vapor density. Gelb and Müller[11] and Martínez-Veracoechea and Müller[13] cut the simulation volume into boxes and determined average coordination numbers of each box then placed the average coordination numbers into an inverse histogram. The maximum repeated values are then used with a cutoff to determine the density of each phase. The resulting procedure has four adjustable parameters for the determination of the phases. These four parameters are the distance cutoff for coordination number, spatial bin size, density bin size for the probability distribution function, and phase cutoffs of the maximum values in the distribution function.

The use of bins presents statistical problems when creating a probability distribution of a local property. One would like to have as many bins as possible to obtain the best statistical representation, but in the limit of very small bins, the resulting density distribution is either 1 or 0 because the bin is either occupied or unoccupied, which presents no useful information regarding the densities of the phases. The other extreme is that in the use of very large bins, the resulting density profile is that of the total system, which provides no useful information on the phase equilibrium. So, the hope is that there exists an intermediate sized bin from which the best VLE data possible can be extracted. The optimal bin size, if it exists at all, is probably a function of thermodynamic state. This problem associated with bins makes the extraction of reliable VLE data from 2ϕMD fraught with effects due to arbitrarily chosen bin-size. These problems are eluded to by Martínez-Veracoechea and Müller.[13] In the literature, these issues have been partially overcome by the use of very large (500 000 particle) simulations.[11,13] It is also important to note that the use of very large systems can also be used combat to finite size effects as the system approaches the critical point.

One other method to determine the bulk vapor and liquid densities is to fit the density profile along the axis normal to the interface to a hyperbolic tangent function.[14] The function contains four adjustable parameters. The use of the hyperbolic tangent function relies upon a planar interface being present, along with no local effects due to obtaining the two-phase system such as explosive boiling, and the center of mass of the liquid droplet remaining stationary. Since the function only allows for planar interfaces, the investigation of densities close to the critical temperature is not an option since there is no guarantee that the interface will be planar. Also, the fitting of the function loses all information about any other local phenomena.

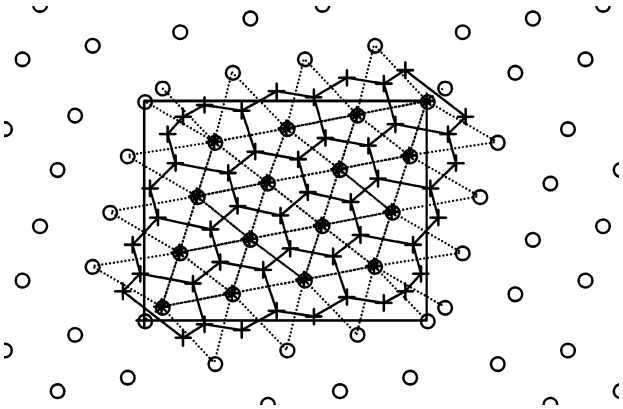

Figure 1. An illustration of a Voronoi tessellation in a two-dimensional, periodic simulation cell. The circles represent the molecules, the dashed lines are the nearest neighbors of each molecule, the ×'s are the vertices which define the subvolume of each molecule, and the solid lines connect the vertices.

To correct the above deficiencies, a method is presented that utilizes Voronoi tessellations (VT) to determine the volume of every particle in the simulation cell. This method is free of all arbitrary choices by the user and can be easily implemented in any system. Furthermore, the method will link the two-phase simulations back to single-phase simulations by the normalized variance of the molecular volume as determined from the Voronoi tessellation. This link will be used as a self-consistency check to ensure that the correct values for the density are obtained, thus removing all arbitrary choices in phase definition. The new method is also capable of giving new insight to the phenomena that occurs as the temperature approaches the critical point.

Voronoi Tessellation

Voronoi tessellations (VT) have wide applications and have been utilized to obtain information pertaining to stellar bodies,[15] free volumes in proteins,[16] crystal deformations,[14] the properties of neurons,[17] and the physics of hard-sphere fluids[18,19] in addition to many other applications.[20] For a thorough reference of the history of VT see the review by Aurenhammer.[15]

VT[14,15,20] is a procedure that takes as input a set of points in a volume (either periodic or bounded) and divides the volume into subvolumes or cells associated with each point, such that all of the volume associated with a point is geometrically closer to that point than to any other. The subvolumes are only a function of the distance to the nearest neighbors of every point. An illustration of this procedure is shown in Figure 1.

Figure 1 shows the resulting subvolumes for a simple periodic system in two dimensions. The dotted lines represent the nearest neighbors around every point, the ×'s are the vertices from the VT defining the subvolume, and finally the solid lines connect the vertices around each point.

When applied to a system at the molecular level, VT leads to a molecular volume for every particle. From this set of molecular volumes, V_n^i, we can obtain, among other statistical properties, the mean molecular volume, $\overline{V_n}$, and the variance of

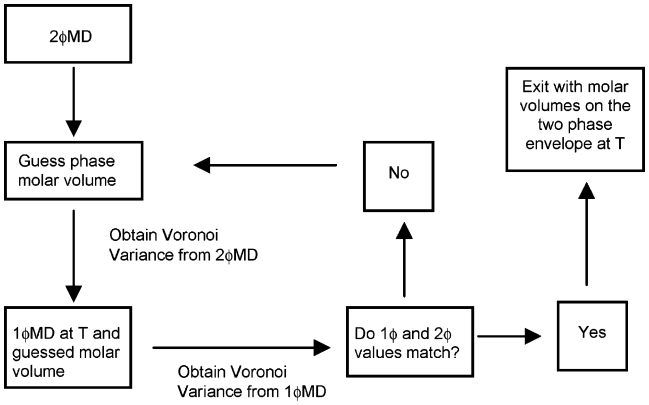

Figure 2. Flow sheet describing the procedure to determine the molar volumes of the vapor and liquid phases at each temperature.

the molecular volume, $\sigma^2_{V_n}$. Each particle is in a Voronoi cell, which in effect is its own custom-sized bin. However, the size of the bin is different for each particle because it is uniquely defined by the VT.

Phase Determination

To locate "bulk liquid" and "bulk vapor" phases within the 2ϕMD simulation, an iterative procedure is used. First, one guesses (i) the upper limit of the average liquid molecular volume so that all molecules with volume less than that limit are defined as liquid and (ii) the lower limit of the vapor molecular volume so that all molecules with volume greater than that limit are defined as vapor. On the basis of these limits, one calculates the liquid statistical measures, $\overline{V_n^L}$ and $\sigma^2_{V_n{}^L}$, based on only those particles defined as liquid. The same procedure applies for the vapor statistical measures, $\overline{V_n^V}$ and $\sigma^2_{V_n{}^V}$.

At this point a self-consistency check must be used to determine the validity of our arbitrarily chosen limits on the molecular density of each phase. This check is simple: two one-phase Molecular Dynamics (1ϕMD) simulations are performed at the same temperature as the 2ϕMD simulation and at the molar volume given by $\overline{V_n^L}$ and $\overline{V_n^V}$. From the 1ϕMD simulations $\sigma^2_{V_n{}^L}$ and $\sigma^2_{V_n{}^V}$ are computed. If the value of $\sigma^2_{V_n{}^L}$ and $\sigma^2_{V_n{}^V}$ from 1ϕMD matches those from 2ϕMD within an acceptable tolerance, then the choice of phase limits was good. Otherwise, one must choose new phase limits and iterate. It is important to point out that each step in the iteration requires a new 1ϕMD simulation (which can be a relatively small system) but not another 2ϕMD simulation (which typically must be much larger), as long as the Voronoi volumes from a set of configurations were saved during the 2ϕMD simulation.

Figure 3 shows an example of this iterative procedure for the liquid and vapor phases, in which the normalized variance of the molecular volume is denoted as $\kappa_1^L \equiv \sigma^2_{V_n{}^L}/\overline{V_n^L}$ and $\kappa_1^V \equiv \sigma^2_{V_n{}^V}/\overline{V_n^V}$. The subscript 1 indicates that this is an averaged single particle property. The 2ϕMD curve was generated from a single simulation, changing only the phase limit until the two lines intersected. The 1ϕMD curve was generated from multiple simulations at varying molar volumes. It can be seen that this combination of 1ϕMD and 2ϕMD provides an unambiguous determination of the phase limits and the corresponding phase properties.

Results and Discussion

As an example system, a simple Lennard-Jones (LJ) fluid is considered, which has been very well studied. The important

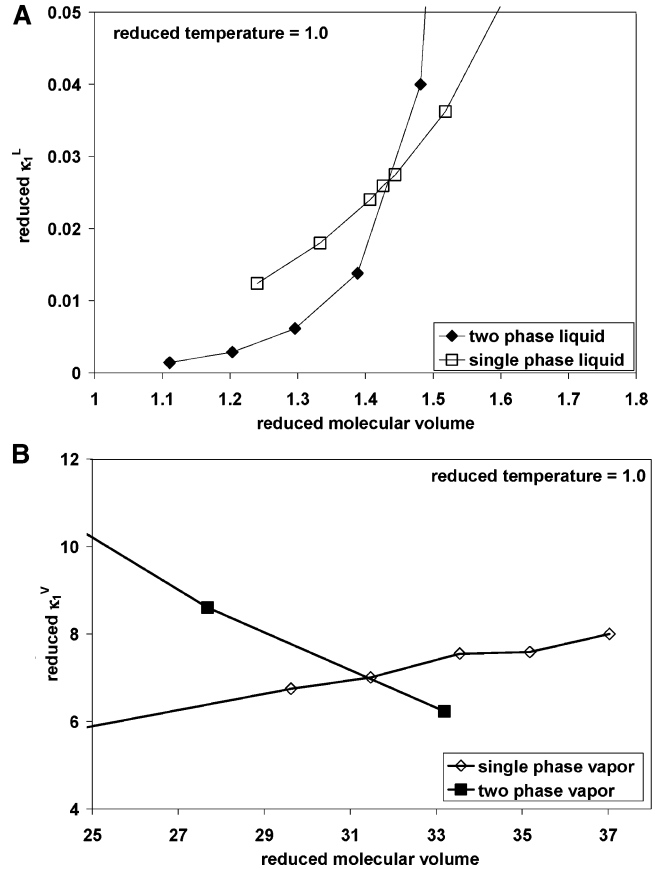

Figure 3. The intersection of the 2ϕ molar volumes and the 1ϕ molar volumes as a function of the normalized variance of the average molar volume denoted by κ_1 for (a) liquid and (b) vapor.

simulation parameters are as follows: 8000 particles were simulated; a cutoff was employed beyond 6 LJ diameters for the interaction potential,[12,21,22] and data were collected for 2 ns after equilibration. The results are presented in reduced Lennard-Jones units.[14]

We include no long-range correction to energy or pressure, because we have a large cutoff distance. There are methods available in the literature to compensate for the long-range corrections in an inhomogeneous system,[23,24] but these methods require there to be a planar interface. The simulations were performed by using TQMD, so it is uncertain if a planar interface would be present. It is also shown from our results that the 2ϕ system has a diffuse and noncontiguous interface, which grows more diffuse as the system approaches the critical temperature.

The simulations were performed on a rigorously tested, in-house designed, parallel MD code. The simulations used a Nose'−Hoover thermostat[25] and a fifth-order Gear Predictor-Corrector.[26,27] The Voronoi analysis was also performed on an in-house designed parallel code, using the properties of Voronoi diagrams mentioned by O'Rourke.[20]

To implement the Voronoi Tessellations in an MD simulation a periodic simulation cell is used with the minimum image convention, the triangulation is performed on the center of mass of Lennard-Jones spheres, and the analysis is performed after the simulation was completed on saved configurations. The speed of the analysis was increased by truncating a sorted neighbor list. The total volume of the simulation cell was used as a check to determine if enough neighbors were used in the analysis. The summation of the individual molecule volumes equals the total simulation volume to machine precision.

To ensure that the simulations were equilibrated, the simulations at low and intermediate temperatures ($T^* = 0.90$ to 1.20)

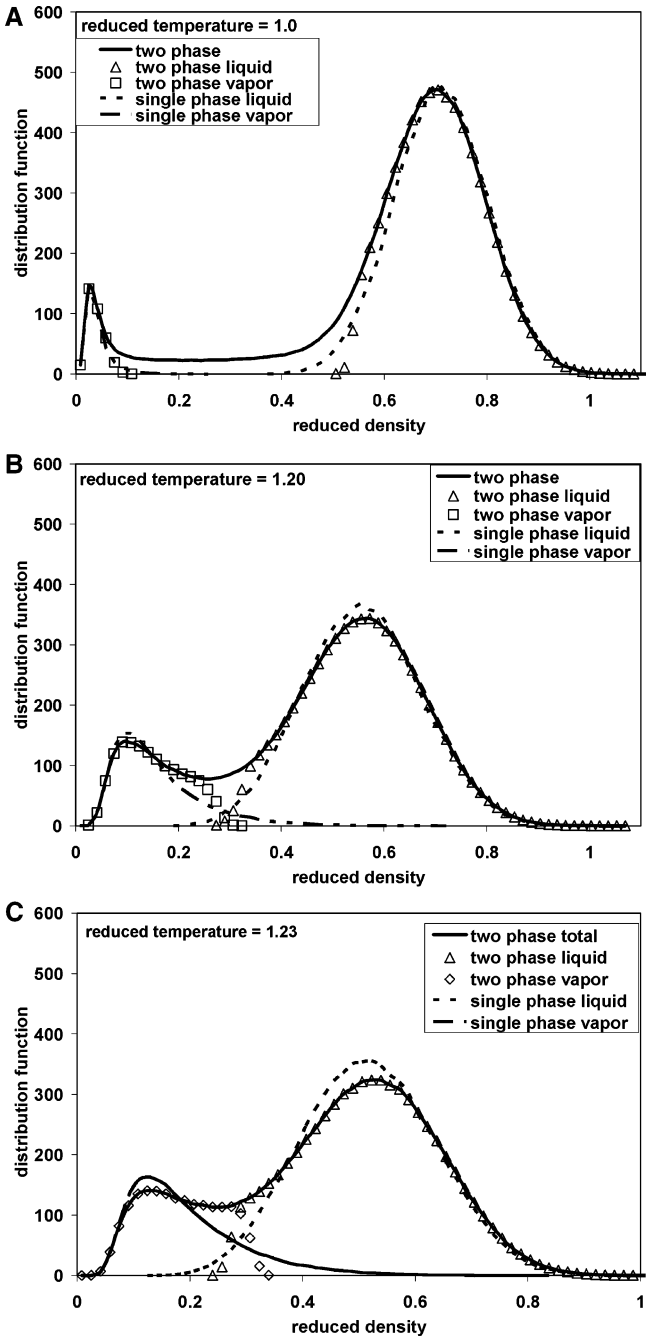

Figure 4. The unnormalized distribution of molecules in the 2ϕ simulation (solid line); the results from the procedure for the liquid (triangles) and vapor (boxes) phases, and the 1ϕ liquid and vapor simulations (dashed lines). Reduced temperature is (a) 1.0, (b) 1.2, and (c) 1.23.

ran for 5.15 ns before data production. The simulations at higher temperatures ($T^* = 1.20$ to 1.27) equilibrated for 8.2 ns and at the highest temperature ($T^* = 1.29$) equilibration lasted for 11.20 ns. The potential energy was monitored throughout the simulation to show if the energy of the system had equilibrated, and the equilibration of particle volumes was determined by monitoring the variance of the Voronoi volume over all particles. In addition, the vapor and liquid densities were calculated via the procedure presented every 0.1 ns, which showed that the densities fluctuated about constant values with time.

In Figure 4, the probability distributions of the molecular density from the converged 1ϕMD and 2ϕMD simulations at various temperatures are shown. All temperatures are below the critical point. Good qualitative agreement is seen between the 1ϕMD and 2ϕMD distributions for the liquid and vapor. It is important to note that the 1ϕMD and 2ϕMD distributions for each phase have the same mean molecular volume and the same variance of the molecular volume. Clearly, the shape of the distributions does not match exactly.

Well below the critical temperature, as shown in Figure 4a, there is a set of molecules that are neither vapor nor liquid, which we can consider as interfacial molecules. Interestingly, as one approaches the critical point, the distributions of the vapor and liquid phases from the independent single-phase simulations overlap. Consequently, in the 2ϕMD simulation at temperatures below but near the critical temperature, the lower density limit of the liquid is less than the upper limit of the vapor. As a result, some particles are considered as both vapor and liquid. In other words, in a near critical fluid, there are liquid regions, vapor regions, and regions that can be considered as both liquid and vapor.

In Figure 5, a series of snapshots are shown of equilibrated 2ϕMD simulations at multiple temperatures, all below the critical point. We color the atoms by phase: particles in the liquid phase are green and particles in the vapor are red. At low temperatures (T less than 1.20), particles that are neither vapor nor liquid are blue. At high temperatures (T greater than 1.20), particles that are both vapor and liquid are blue. We see that the use of VT allows for us to define vapor and liquid phases *that are not contiguous*. This is an important advantage of using VT to define local density rather than the conventional use of spatial bins because as one nears the critical point, one does not expect to find contiguous phases. This presents the possibility that the use of VT will allow this simulation technique to continue to provide good VLE data closer to the critical point than other methods.

In Figure 5a−c, we see that far below the critical temperature, there are bulk liquid and vapor sections. The interfacial atoms are located primarily at the bulk interface but also are scattered through the bulk phases. This scattering of interfacial particles (by defining the interface as neither bulk vapor nor bulk liquid) is a result of the VT procedure. Were one to use spatial bins and define all molecules in the predominantly green region as liquid or those in the predominately red region as vapor, one would obtain higher vapor densities and lower liquid densities. This procedure suggests that "interfacial" particles are concentrated at but not limited to the bulk interface. As the temperature is increased in Figure 5d−f, we see that there are no longer any interfacial atoms. All atoms are either bulk liquid, bulk vapor, or both bulk liquid and bulk vapor. It can be seen that those atoms with molecular volumes corresponding to both bulk liquid and bulk vapor are not concentrated at the interface of the predominately liquid and predominately vapor regions, but rather are scattered throughout the system.

In Figure 6, we show the vapor−liquid phase diagram for this system. In the plot, we compare (i) the result of our method, (ii) the results from GEMC simulation,[13] (iii) and results from a 32-parameter EOS fit to extensive MD simulation data.[28] We see that our new method provides excellent agreement with GEMC. We also see that our algorithm containing 2ϕMD and 1ϕMD simulations allows one to obtain properties much closer to the critical point. GEMC has difficulty simulating close to the critical temperature because the identity of the liquid and vapor phases can swap during the simulation.[6] Near the critical point, there is non-negligible disagreement between the simulation results (2ϕMD or GEMC) and the LJ-EOS. Since the two independent simulation methods agree, we believe that this disagreement between simulation and EOS is likely due to

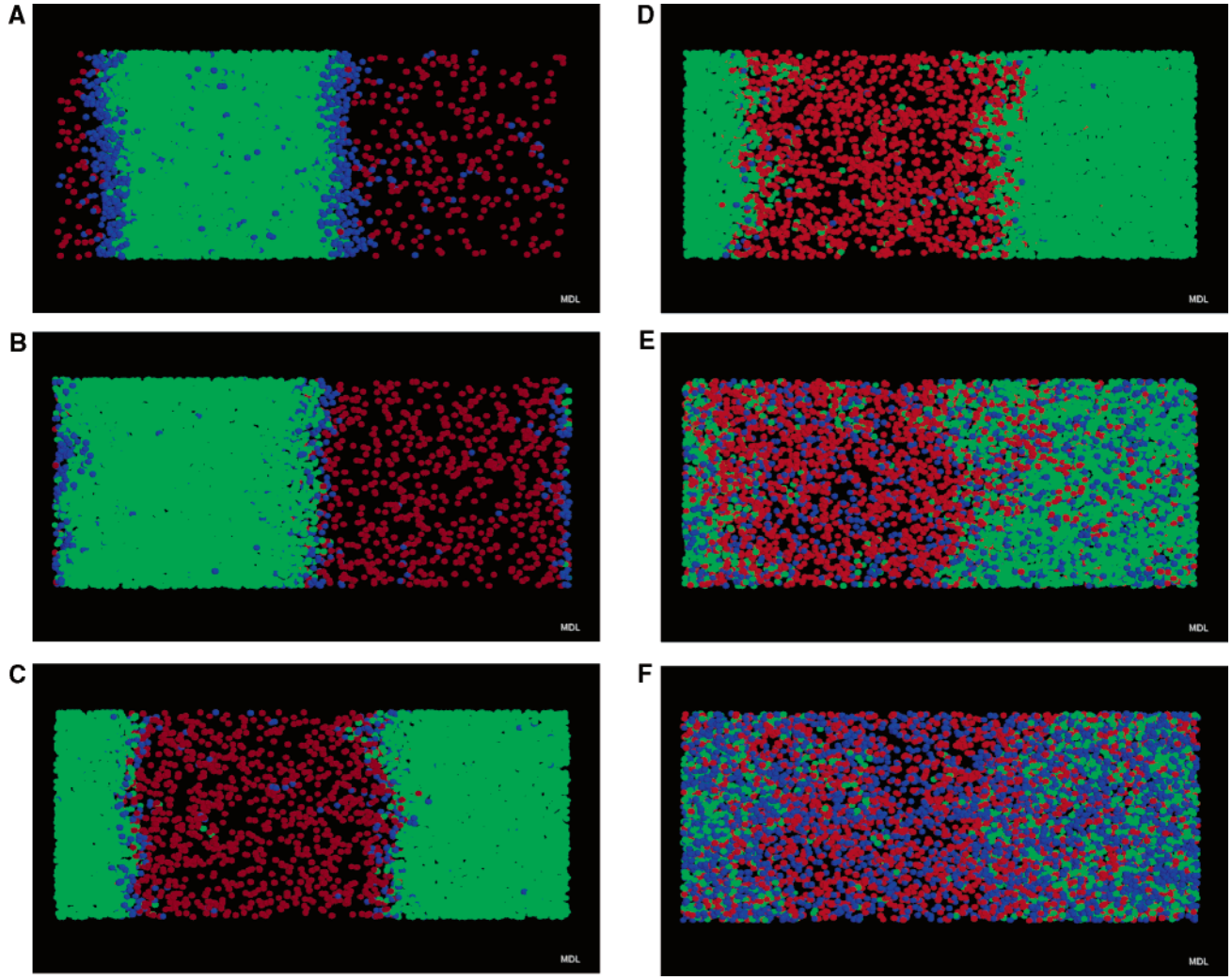

Figure 5. A snapshot of the final configuration for a reduced temperature of (a) 1.0, (b) 1.10, (c) 1.15, (d) 1.20, (e) 1.27, and (f) 1.29. In all plots, green represents the liquid molecules and red represents the vapor molecules. At temperatures at and below 1.20 blue molecules are interfacial (neither liquid nor vapor) and at the high temperatures (above 1.20) blue molecules are both vapor and liquid.

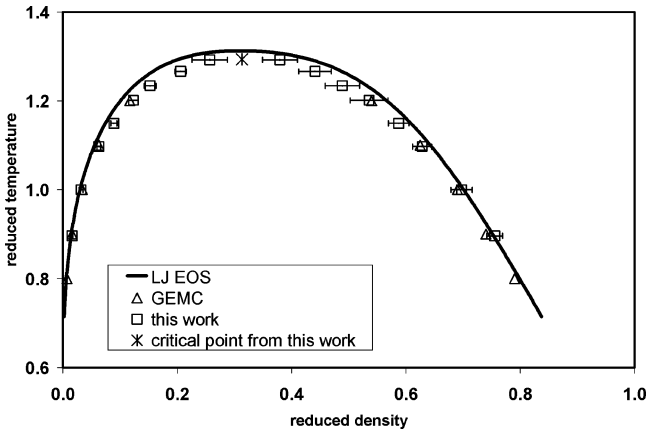

Figure 6. The phase diagram. The solid line is the Lennard-Jones Equation of State (EOS);[28] the triangles are results from Gibbs Ensemble Monte Carlo;[13] and the boxes are the results from this work The critical point as determined from the fit from this work is designated with an asterisk.

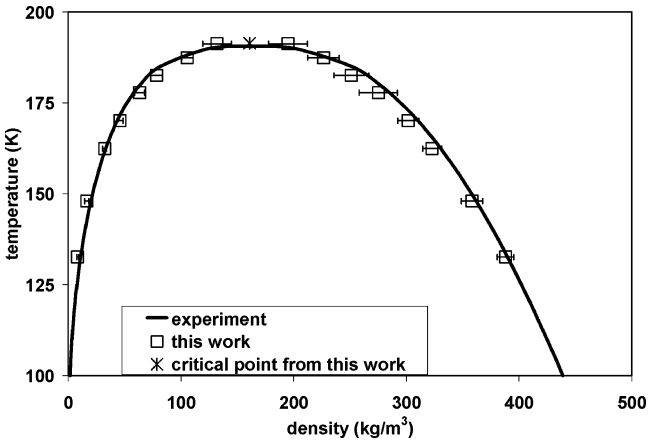

Figure 7. The phase diagram. The solid line shows the experimental data for methane,[29] and the boxes are the results from this work.

limitations in the LJ-EOS based on the quality of simulation data to which it was fit.

Finally, Figure 7 presents a comparison between our results from the algorithm containing 2ϕMD and 1ϕMD simulations with experimental results for methane,[29] which is reasonably well approximated as a Lennard-Jones fluid. While one might expect simulation results of a LJ fluid to match an EOS fit to simulation data better than experiment, here we observe the contrary behavior.

The critical temperature of this system is 1.293 and the critical density is 0.313 in reduced units as determined by the law of rectilinear diameters and by the Ising scaling with the classical critical exponent of 0.32.[6,30,31] The critical temperature of the Lennard-Jones EOS is 1.316 and the critical density is 0.304.

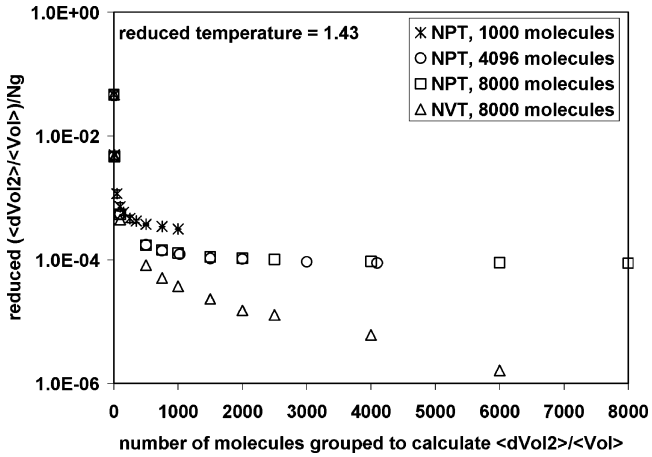

Figure 8. The normalized variance per particle as a function of cluster size for 3 single-phase simulations in the NpT ensemble with N = 1000 (asterisks), 4096 (circles), and 8000 (boxes) particles and for 1 single-phase simulation in the NVT ensemble with $N = 8000$ (triangles). N_g is the group size.

The resulting percentage errors are 1.7% for the critical temperature and 3.0% for the critical density. The LJ EOS may overestimate the critical point and coexisting densities at high temperatures. There were only two sets of data used to perform the fit in the critical regime.[28] One of the sets of data was the NPT + test particle method of Lofti.[7] It is possible that the Lofti data overpredicted the breadth of the phase envelope because it is very difficult to simulate in the NPT ensemble along the two-phase region and simulated just outside the two-phase region. This is because the system can drift to vapor from liquid and liquid to vapor. If one uses the LJ EOS to calibrate the arbitrary phase definition, one can find better agreement with the LJ EOS, resulting in a systematic deviation from our simulation results, which are free of arbitrary choices.

If methane is considered as the fluid with σ= 3.73 Å and ϵ = 148 K[12] the resulting critical temperature is 191.4 K and the critical density is 161.0 kg·m^{-3}. The accepted experimental value for the critical temperature of methane is 190.5 K and the critical density is 162.6 kg·m^{-3}. So our percent error to the experimental critical temperature is 0.4% and our percent error to the critical density is 1.1%. It is felt that the good agreement seen as compared to the experimental data validates our conclusions concerning the LJ EOS.

We should point out that we can use a small number of particles (8000) with VT as compared to 500 000 particles used to counter the statistical problems associated with spatial bins.[13] Another reported advantage of the large system size is that it combats the system size effects that can occur as the temperature approaches the critical point. Our new method does not appear to be as affected by finite size effects, because phase definition is based on highly localized properties (single-particle molecular volume and single-particle molecular volume variance).

This technique is directly extendable to the phase equilibrium of mixtures, in which limits for the density of each species in each phase must be iteratively determined. It is also directly applicable to polyatomic fluids, since the VT can be applied to individual atoms and then summed over all atoms in a molecule to yield the molecular volume.

Equivalency of κ_1 Across Simulations and Ensembles. Since κ_1 is being used as a criterion for defining the phases, it is important to establish that the measured value of κ_1 is independent of the size of the system and the ensemble in which the simulation is performed. In Figure 8 the normalized variance per particle as a function of cluster size for 3 single-phase simulations in the NpT ensemble with N = 1000, 4096, and 8000 particles and for 1 single-phase simulation in the NVT ensemble with N = 8000 particles is plotted. Clusters were formed by randomly grouping molecules (without any regard for position). Thus a simulation with $N = 8000$ had 8000 clusters of size 1 and 2 clusters of size 4000.

The crucial point in Figure 8 is that for all simulations, regardless of size or ensemble, the value of the normalized variance per particle is the same for a cluster size of one. Therefore the single-particle property, κ_1, is independent of system size and ensemble. This is important because the phase criteria is based upon a comparison of κ_1 from a 1ϕMD simulation in the NVT ensemble of N = 1000 with κ_1 from a 2ϕMD simulation, where the volume and number of particles in each phase varies from one configuration to the next.

At cluster sizes larger than one, the normalized variance per particle is a function of system size and ensemble. If we take this to the limit where we have 1 cluster composed of all of the particles in the simulation, then we find that variance in the NVT simulation goes to zero, as it must since the total volume is constant. The variance in the NpT ensemble goes to a value independent of system size, once a minimum system size is used. This is consistent with fluctuation theory, which states that the isothermal compressibility, given by[14]

$$\beta_T = \frac{1}{k_B T} \frac{\langle \delta \mathrm{Vol}^2 \rangle_{\mathrm{NPT}}}{\langle \mathrm{Vol} \rangle} \tag{1}$$

is a function of the normalized variance of the volume per particle.

Part of our motivation in choosing the mean and the variance of the Voronoi volume as criteria for the phase definitions in 2ϕMD simulations was the fact that these two properties are local properties. The normalized variance of the single-particle molecular volume, κ_1, and the isothermal compressibility from fluctuation theory share the same functional form, but they are not representative of the same property (since the former assumes a cluster size of 1 and the latter a cluster size of N). It is nevertheless interesting to note that the bulk isothermal compressibility is itself a highly localized function, as evidenced by the fact that, in the Ornstein−Zernike closure, the isothermal compressibility is strictly a function of the short-ranged direct correlation function.[30]

Conclusions

A new method is presented to account for the statistical problems associated with the use of bins in 2ϕMD simulations. The new method utilizes Voronoi tessellations to obtain the molecular volumes for every particle simulated. The resulting mean and variance of the molecular volumes are then used to self-consistently determine the phases. There is excellent agreement between this work and GEMC simulations far from the critical point, where GEMC data are available. We have excellent agreement with experimental results up to and including the critical point. The new algorithm also allows for new insight as the system approaches the critical temperature since at every instant in time one can know if a molecule is in the liquid or vapor phases regardless of the location of the interface. We see that well below the critical temperature, some particles are neither liquid nor vapor. These interfacial particles are primarily but not exclusively concentrated at the bulk interface. However, as we approach the critical point, some particles are necessarily both liquid and vapor. These interfacial particles are distributed through the system.

Acknowledgment. The authors gratefully acknowledge the financial support of the Office of Fossil Energy of the U.S. Department of Energy (DOE). Through the UT Computational Science Initiative, this research project used resources of the Center for Computational Sciences at Oak Ridge National Laboratory, which is supported by the Office of Science of the DOE under Contract DE-AC05-00OR22725.

References and Notes

(1) Ladd, A. J. C.; Woodcock, L. V. *Mol. Phys.* **1978**, *36*, 611.
(2) Chapela, G. A.; Saville, G.; Thompson, S. M.; Rowlinson, J. S. *Faraday Trans.* **1977**, *73*, 1133.
(3) Holcomb, C. D.; Clancy, P.; Thompson, S. M.; Zollweg, J. A. *Fluid Phase Equil.* **1992**, *75*, 185.
(4) Holcomb, C. D.; Clancy, P.; Thompson, S. M.; Zollweg, J. A. *Fluid Phase Equil.* **1993**, *88*, 303.
(5) Panagiotopoulos, A. Z. *J. Phys.*: *Condens. Matter* **2000**, *12*, R25.
(6) Frenkel, D.; Smit, B. *Understanding Molecular Simulation From Algorithms to Applications*, 2nd ed.; Academic Press: San Diego, CA, 2002.
(7) Lofti, A.; Vrabec, J.; Fischer, J. *Mol. Phys.* **1992**, *76*, 1319.
(8) Widom, B. *J. Chem. Phys* **1963**, *39*, 2808.
(9) Pontoff, J. J.; Panagiotopoulos, A. Z. *J. Chem. Phys.* **1998**, *109*, 10914.
(10) Pe'rez-Pellitero, J.; Ungerer, P.; Orkoulas, G.; Mackie, A. D. *J. Chem. Phys.* **2006**, *125*, 054515.
(11) Gelb, L. D.; Muller, E. A. *Fluid Phase Equil.* **2002**, *203*, 1.
(12) Pamies, J. C.; McCabe, C.; Cummings, P. T.; Vega, L. F. *Mol. Simul.* **2003**, *29*, 463.
(13) Martinez-Veracoechea, F.; Muller, E. A. *Mol. Simul.* **2005**, *31*, 33.
(14) Allen, M. P.; Tildesley, D. J. *Computer Simulation of Liquids*; Clarendon Press: Oxford, UK, 1989.
(15) Aurenhammer, F. *ACM Comput. Surveys* **1991**, *23*, 345.
(16) Gerstein, M.; Tsai, J.; Levitt, M. *J. Mol. Biol.* **1995**, *249*, 955.
(17) Duyckaerts, C.; Godefroy, G. *J. Chem. Neuroanat.* **2000**, *20*, 83.
(18) Kumar, V. S.; Kumaran, V. *J. Chem. Phys.* **2005**, *123*, 074502.
(19) Kumar, V. S.; Kumaran, V. *J. Chem. Phys.* **2005**, *123*, 114501.
(20) O'Rourke, J. *Computational Geometry in C*; Cambridge University Press: New York, 1994.
(21) Alejandre, J.; Tildesley, D. J.; Chapela, G. A. *J. Chem. Phys.* **1995**, *102*, 4574.
(22) Trokhymchuk, A.; Alejandre, J. *J. Chem. Phys.* **1999**, *111*, 8510.
(23) Duque, D.; Vega, L. F. *J. Chem. Phys.* **2004**, *121*, 8611.
(24) Duque, D.; Pamies, J. C.; Vega, L. F. *J. Chem. Phys.* **2004**, *121*, 11395.
(25) Nose', S. *J. Chem. Phys* **1984**, *81*, 511.
(26) Gear, C. W. *The Numerical Integration of Ordinary Differential Equations of Various Orders*; Argonne National Laboratory, Argonne, IL, 1966.
(27) Gear, C. W. *Numerical Initial Value Problems in Ordinary Differential Equations*; Prentice Hall, Inc.: Englewood Cliffs, NJ, 1971.
(28) Johnson, J. K.; Zollweg, J. A.; Gubbins, K. E. *Mol. Phys.* **1993**, *78*, 591.
(29) Setzmann, U.; Wagner, W. *J. Phys. Chem. Ref. Data* **1991**, *20*, 1061.
(30) Rowlinson, J. S. *Liquids and Liquid Mixtures*; Butterworth & Co: London, UK, 1969.
(31) Rowlinson, J. S.; Widom, B. *Molecular Theory of Capillarity*; Oxford University Press: New York, 1982.
(32) McQuarrie, D. A. *Statistical Mechanics*; University Science Books: Sausalito, CA, 2000.